INTERNAL SHEAR STRENGTH OF THREE GEOSYNTHETIC CLAY LINERS

The attached paper presents the results of internal shear testing of three GCL products: GCL-A (Claymax 200RW, an unreinforced GCL); GCL-B (Claymax 600SP, a discontinued stitch-bonded GCL); GCL-C (Bentomat ST, a standard needlepunch-reinforced GCL). The study assessed the effects of specimen hydration, displacement rate, and normal load on the measured internal shear strength.

A four-day, two-stage hydration procedure was investigated, where the GCL was initially hydrated under low (or no) normal load for 2 days, and then hydrated/consolidated under the test normal load for an additional 2 days. Measurements collected during the two-stage hydration (Figures 4b, 4d, and 4f) showed that, in many instances, pore pressures within the bentonite did not fully dissipate until after 48 hours of consolidation. These results state the importance of proper hydration/consolidation in ensuring that accurate shear strength results are obtained, particularly at high normal loads. If a sample is sheared before it is fully consolidated, positive pore pressures may develop within the bentonite, reducing the actual effective stress acting on the sample, likely resulting in a lower measured shear strength.

Changes in shear displacement rate (0.01, 0.1, 1, and 10 mm/min) resulted in slight decreases (3 to 5%) in peak shear strength.

As might be expected, the unreinforced Claymax showed the lowest peak shear strength (and smallest decrease in post-peak strength), while Bentomat showed the highest peak shear strength (and highest decrease in post-peak strength). The residual (large displacement) shear strength values appeared independent of product type, and were consistent with past test data for fully hydrated sodium bentonite (ϕ = 4.0 degrees). Although the residual strengths were comparable, there were significant differences in the amount of displacement needed to reach these strengths. Claymax reached its residual strength after only 1.5 mm of displacement, while Bentomat, due to the reinforcing needlepunched fibers, reached its residual strength at 17 to 23 mm of displacement. Examination of the sheared Claymax specimens revealed that the failure plane was consistently located at the woven geotextile/bentonite interface. The Bentomat specimens primarily failed as nonwoven reinforcing fibers were pulled through the woven geotextile.

800.527.9948 Fax 847.577.5566

INTERNAL SHEAR STRENGTH OF THREE GEOSYNTHETIC CLAY LINERS

By Patrick J. Fox,[1] Michael G. Rowland,[2] and John R. Scheithe,[3] Associate Members, ASCE

ABSTRACT: A study of the internal shear strength of adhesive-bonded, stitch-bonded, and needle-punched geosynthetic clay liners (GCLs) is presented. Tests were performed using a large direct shear machine capable of measuring peak and residual (or near residual) shear strengths. For each product, failure occurred at the woven geotextile/bentonite interface and excess pore pressures remained zero on the failure plane during shear. The peak shear strength of the needle-punched GCL increased significantly with increasing normal stress because of the frictional connection of the reinforcing fibers. The peak shear strengths of the adhesive-bonded and stitch-bonded GCLs showed smaller corresponding increases. The residual shear-strength failure envelope was essentially independent of product type. A two-stage procedure for specimen hydration is described, which reduced the required in-machine hydration time to reach equilibrium conditions. For the reinforced products, small decreases in peak and residual shear strengths were observed with decreasing displacement rate. The findings of the study have implications for the design of facilities incorporating GCLs and for the manufacturing and shear-strength testing of GCL products.

INTRODUCTION

Geosynthetic clay liners (GCLs) are manufactured hydraulic barriers consisting of bentonite clay bonded to a layer, or layers, of geosynthetic material. Stability of GCLs is an important consideration for design because of the low shear strength of the bentonite after hydration. Unreinforced GCLs are held together by chemical adhesives and, once hydrated, provide relatively low resistance to shear. For higher shear-strength applications, reinforced products are required in which the carrier geosynthetics are connected by stitches or needle-punched fibers that transmit shear stress across the bentonite layer. In either case, internal shear strength of the GCL and interface shear strengths between the GCL and adjacent materials need to be considered for stability analysis. Internal GCL shear strengths generally are obtained from laboratory direct shear tests and are dependent on many variables, including product type, hydration fluid, hydration time, shear rate, shear displacement, normal stress and drainage conditions during hydration and shear, and other equipment-specific factors (e.g., specimen gripping system). As such, design values of internal GCL shear strength should be measured on a product-specific basis under conditions closely simulating those expected in the field.

A study of the internal shear strength of adhesive-bonded, stitch-bonded, and needle-punched GCLs is presented in this paper. Laboratory tests were performed using a large direct shear apparatus capable of measuring peak and residual (or near residual) shear strengths. Testing procedures are described and results are presented for each GCL product. Comparison of the test data gives insight with regard to mechanisms of internal shear-strength development as a function of normal stress and horizontal displacement. In addition, the results of separate studies on specimen hydration procedure and the effect of displacement rate on measured shear strength are presented. Finally, implications of the research findings to the design of waste-containment facilities and other facilities incorporating GCLs and to the manufacturing and testing of GCL products are discussed.

LABORATORY TESTING PROGRAM

Materials

Three commercial GCL products, representing the three principal types of GCL construction, were chosen for the experimental program (Table 1). Each product contains approximately 5 kg of sodium bentonite per square meter of GCL and typically is 5–15 mm thick in the hydrated state. GCL-1 [Claymax 200RW, Colloid Environmental Technologies Co. (CETCO), Arlington Heights, Ill.] was an unreinforced adhesive-bonded GCL in which granular bentonite is held between two woven slit-film polypropylene geotextiles, each having a mass/area of 109 g/m^2. GCL-2 (Claymax 600SP, CETCO) was a reinforced product in which granular bentonite is held between two woven slit-film polypropylene geotextiles (109 g/m^2) that are stitch-bonded together. The lines of stitching run in the machine direction with a transverse spacing of 102 mm. GCL-2 also incorporates a 0.10 mm thick polyethylene geomembrane laminated to the inside of one of the woven geotextiles. GCL-3 (Bentomat ST, CETCO) was a reinforced product in which granular bentonite is held between a woven slit-film polypropylene geotextile (109 g/m^2) and a nonwoven needle-punched polypropylene geotextile (204 g/m^2). To provide reinforcement, polypropylene fibers from the nonwoven geotextile are needle-punched through the bentonite and the woven geotextile.

Equipment

Direct shear tests were performed on large (406 × 1,067 mm) rectangular GCL specimens using a pullout shear machine (Fox et al. 1997). A scale drawing of the machine is shown in Fig. 1. A GCL specimen is sheared between the underside of a horizontal pullout plate and the floor of the test chamber, each of which is covered with an aggressive gripping surface (modified metal connector plates used for wood-truss construction). The shearing surfaces permit drainage of the specimen on both sides and enforce uniform shear strain at failure without clamping the ends of the carrier geosynthetics. The maximum horizontal displacement of the pullout plate is 203 mm. The shearing system is powered by two stepper motors, which rotate two lead screws and draw the pullout plate forward at a constant rate of displacement. Normal stress is provided by two air bags, which rest on an overlying stationary load plate. Between the load plate and the pullout plate, a

[1]Assoc. Prof., School of Civ. Engrg., Purdue Univ., West Lafayette, IN 47907.

[2]Staff Engr., BBC&M Engrg., Inc., Dublin, Ohio 43016; formerly, Grad. Res. Asst., School of Civ. Engrg., Purdue Univ., West Lafeyette, IN.

[3]Engr., Traylor Bros., Inc., Evansville, IN 47716; formerly, Grad. Res. Asst., School of Civ. Engrg., Purdue Univ., West Lafayette, IN.

Note. Discussion open until March 1, 1999. To extend the closing date one month, a written request must be filed with the ASCE Manager of Journals. The manuscript for this paper was submitted for review and possible publication on June 4, 1997. This paper is part of the ***Journal of Geotechnical and Geoenvironmental Engineering***, Vol. 124, No. 10, October, 1998. ©ASCE, ISSN 1090-0241/98/0010-0933–0944/$8.00 + $.50 per page. Paper No. 15927.

TABLE 1. GCL Products Tested for Experimental Program

GCL Product (1)	Upper geotextile (2)	Lower geotextile (3)	Reinforcement (4)
GCL-1 (Claymax 200RW)	Polypropylene slit-film woven (109 g/m^2)	Polypropylene slit-film woven (109 g/m^2)	None
GCL-2 (Claymax 600SP)	Polypropylene slit-film woven (109 g/m^2)	Polypropylene slit-film woven (109 g/m^2) with a 0.10 mm thick polyethylene geomembrane laminate	Stitch-bonded, 102 mm on center
GCL-3 (Bentomat ST)	Polypropylene slit-film woven (109 g/m^2)	Polypropylene needle-punched nonwoven (204 g/m^2)	Needle-punched throughout

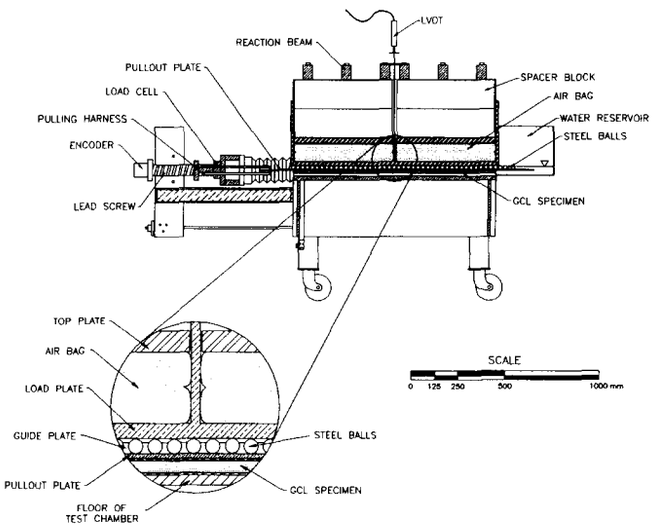

FIG. 1. Pullout Shear Machine

layer of free-rolling stainless steel balls reduces the shear stress due to friction to 0.26% of the applied normal stress. Volume change of a GCL specimen is obtained by measuring vertical displacement at the midpoint of the load plate with a linear variable differential transformer. Pore pressures are measured at two locations inside each specimen using thin stainless steel needles. One needle is placed within the bentonite to measure internal pore pressure. A second needle is placed at the interface between the bentonite and the top geotextile. This interface constituted the failure surface for the GCL products tested in this study. Specimens are hydrated from a water reservoir at the rear of the machine through a network of drainage channels behind both shearing surfaces. The water level is maintained approximately 25 mm above the top of a GCL specimen. An automated process control and data acquisition system controls machine operation and data collection for the hydration and shearing stages of each test.

The pullout shear machine offers the following advantages for GCL shear-strength testing: (1) large specimen size reduces boundary effects and produces more representative shear-strength measurements; (2) specimens can be sheared under a large range of normal stress; (3) residual (or near residual) shear strengths are measured in one direction without requiring shear reversals; (4) the specimen gripping system enforces uniform shear strain at failure without clamping the carrier geosynthetics to the shearing surfaces; and (5) unlike the upper or lower portion of a split-box machine, the applied normal stress does not translate across the specimen during shear.

Procedures

Peel Tests

Peel tests were used to measure the relative strength of needle-punched reinforcement for GCL-3. The procedure was performed on specimens in their as-received moisture condition and was similar to that specified by ASTM D 4632 (ASTM 1997) for grab strength of geotextiles. Three peel test specimens (102 × 254 mm) were cut adjacent to the end of a direct shear test specimen with the long sides parallel to the direction of shear. For tests in which the supply of material was limited, three peel specimens were cut for a GCL roll. The geosynthetics at one end of each peel specimen were separated and clamped to wide-width testing grips, and the specimen was peeled apart at a displacement rate of 305 mm/min. The peel strength (F_p) for a direct shear specimen was taken as the average measured tensile force from the three corresponding peel tests. Used primarily for manufacturing quality control, peel strength has been correlated with internal shear strength of needle-punched GCLs (Heerten et al. 1995; Richardson 1997).

Early in the testing program, peel tests also were performed on specimens of GCL-2 to obtain a relative strength measurement of the stitch-bonded reinforcement. However, during these tests, stitches tended to group together and then break suddenly, producing a highly variable measured tensile force. As a result, a single peel strength could not be obtained for these specimens and peel testing was discontinued for GCL-2. This finding is consistent with manufacturing quality control guidelines presented by Koerner (1997), which recommend peel testing only for needle-punched GCLs.

Specimen Hydration and Shear

A 4-day, two-stage specimen hydration procedure was used for this study, which reduced the required in-machine hydration time for direct shear tests. The as-received water content of each GCL roll was determined first. GCL specimens then were cut parallel to the machine direction such that one carrier geotextile measured 406 × 1,270 mm and the other measured 406 × 1,067 mm. For the first stage of hydration, each specimen was placed in a shallow pan and sufficient tap water was added to bring the specimen to the estimated final water content for the test. These water content values were obtained from previous direct shear tests using the same GCL products. After water was added, specimens were covered to prevent evaporation and allowed to cure for 2 days. During this time, a 1-kPa normal stress was applied to specimens of GCL-1 and GCL-2 to minimize nonuniform swelling. For GCL-3, uniform hydration was achieved without applied normal stress because of the in-plane transmissivity of the nonwoven geotextile and the additional confinement provided by the reinforcing fibers.

After the first stage of hydration was completed, two pore pressure needles were inserted into the end of each GCL specimen. Care was taken to minimize disturbance to the reinforcement for specimens of GCL-2 and GCL-3 during this procedure. To begin the second stage of hydration, specimens were placed in the shear machine such that the longer geotextile was in contact with the pullout plate. For GCL-2 and GCL-3, the woven geotextile/laminated geomembrane and the nonwoven geotextile, respectively, were placed facing down. Normal stress was applied and specimens were hydrated for an additional 2 days. Vertical displacement and pore pressure measurements were recorded during the second hydration stage. For comparison, two additional tests were performed without the first hydration stage to assess the impact of hydration procedure on measured shear strength.

Once the second stage of hydration was completed, GCL

specimens were sheared at a constant displacement rate of 0.1 mm/min to a final displacement between 180 and 203 mm. Additional tests were conducted at 0.01, 1, and 10 mm/min to measure the effect of displacement rate on measured shear strength. During shear, the longer geotextile of each specimen was drawn into the test chamber with the pullout plate. Since failure occurred at the woven geotextile/bentonite interface for these products (see later discussion), failure surface area remained constant and an area correction was not needed for the normal and shear stresses. After shearing was completed, specimens were removed from the machine, the mode of failure was noted, and five water content measurements were taken from each. Water contents were calculated for each GCL product as a whole (i.e., without subtracting the weight of geosynthetics from the weight of solids).

RESULTS

Table 2 provides a summary of the testing program and results. In all, 34 direct shear tests were conducted. The variables for the testing program included product type, peel strength (for GCL-3), hydration procedure, normal stress, shear direction (for GCL-2), and horizontal displacement rate.

Hydration

The effectiveness of the two-stage specimen hydration procedure was first investigated. Two tests were performed for each reinforced product (GCL-2 and GCL-3) at a normal stress (σ_n) of 37.8 kPa. The tests were identical except that one specimen of each product was not hydrated prior to placement in the shear machine and one specimen was hydrated using the two-stage procedure described earlier. Fig. 2 shows the vertical displacement and internal pore pressure measurements for each specimen during hydration under the applied normal stress. Specimens hydrated using the two-stage procedure approached equilibrium more rapidly than specimens placed in the shear machine at the as-received water content. Large internal pore pressures were measured initially because the specimens were inundated during test setup (to remove air and facilitate drainage through the shearing surfaces). A small initial excess pore pressure ($\leq$6.9 kPa) also was measured typically at the woven geotextile/bentonite interface, which dissipated in 30 min or less and remained zero thereafter. After the second stage of hydration was completed, the specimens were sheared at a horizontal displacement rate of 0.1 mm/min. The shear stress (τ) versus horizontal displacement (δ) curves, shown in Fig. 3, are nearly identical for each product.

Figs. 2 and 3 suggest that the two-stage hydration procedure reduces the in-machine hydration time required to reach equilibrium and has no significant impact on measured shear strength. This is consistent with a study reported by the U.S. Environmental Protection Agency (1996) in which the shear strength of an unreinforced GCL was found to be essentially constant for hydration times ranging from 24 to 72 h. Re-

TABLE 2. Testing Program and Results

Product type (1)	Peel strength, F_p (N) (2)	Hydration time, 1st stage/2nd stage (day) (3)	Normal stress, σ_n (kPa) (4)	Horizontal displacement rate (mm/min) (5)	Peak shear strength, t_p (kPa) (6)	Horizontal displacement at t_p (mm) (7)	Residual shear strength, t_r (kPa) (8)	Horizontal displacement at 1.1t_r (mm) (9)	Avg. final water content,[a] w_f (%) (10)
GCL-1	—	2/2	6.9	0.1	3.6	2.4	1.7	83.8	273
GCL-1	—	2/2	24.0	0.1	8.5	1.5	3.8	103.8	194
GCL-1	—	2/2	37.8	0.1	12.0	1.5	5.0	103.4	189
GCL-1	—	2/2	72.2	0.1	18.3	1.5	7.3	113.6	148
GCL-1	—	2/2	141	0.1	28.7	1.4	13.3	69.2	149
GCL-1	—	2/2	279	0.1	52.7	1.6	22.2	116.9	105
GCL-2	—	2/2	24.0	0.1	73.5	63.1	4.7	173.4	188
GCL-2	—	2/2	37.8	0.1	68.6	53.0	6.2	169.0	163
GCL-2	—	0/2	37.8	0.1	64.9	47.2	6.3	145.8	157
GCL-2	—	2/2	72.2	0.01	74.1	49.4	8.3	126.1	136
GCL-2	—	2/2	72.2	0.01	81.8	53.5	8.5	123.4	129
GCL-2	—	2/2	72.2	0.1	86.3	46.5	9.8	133.3	135
GCL-2	—	2/2	72.2	0.1	92.5	51.0	9.3	146.4	140
GCL-2	—	2/2	72.2[b]	0.1	47.5	31.1	9.1	103.8	147
GCL-2	—	2/2	72.2[b]	0.1	53.6	32.7	9.6	101.3	149
GCL-2	—	2/2	72.2	1	81.3	45.7	10.4	142.0	131
GCL-2	—	2/2	72.2	10	94.9	43.5	10.9	136.3	126
GCL-2	—	2/2	72.2	10	86.8	40.8	10.0	133.2	142
GCL-2	—	2/2	141	0.1	83.2	39.7	15.6	114.6	115
GCL-2	—	2/2	279	0.1	91.4	44.6	26.6	102.5	81
GCL-2	—	2/2	279	0.1	94.9	45.6	—	—	75
GCL-3	160	2/2	37.8	0.1	122.7	25.8	5.0	125.3	198
GCL-3	180	2/2	72.2	0.1	160.3	21.5	9.0	108.5	158
GCL-3	150	2/2	141	0.1	184.8	22.9	13.8	98.9	138
GCL-3	160	2/2	279	0.1	276.8	23.2	22.0	111.1	101
GCL-3	85[c]	2/2	17.1	0.1	62.4	23.5	3.8	100.1	228
GCL-3	85[c]	2/2	37.8	0.1	75.8	16.5	5.6	107.6	191
GCL-3	85[c]	2/2	72.2	0.1	114.5	16.9	9.3	81.8	137
GCL-3	85[c]	2/2	141	0.1	169.3	20.4	—	—	121
GCL-3	110	0/2	37.8	0.1	93.3	21.4	5.8	109.1	181
GCL-3	110	2/2	37.8	0.1	88.2	21.0	5.2	124.0	184
GCL-3	160[c]	2/2	72.2	0.01	139.3	22.4	9.6	78.6	162
GCL-3	160[c]	2/2	72.2	1	147.9	23.2	9.5	116.3	160
GCL-3	160[c]	2/2	72.2	10	156.1	21.9	9.7	129.9	161

[a]Coefficients of variation ranged from 1.6 to 14.3%.
[b]Specimen sheared in reverse direction.
[c]Average value for roll (three specimens).

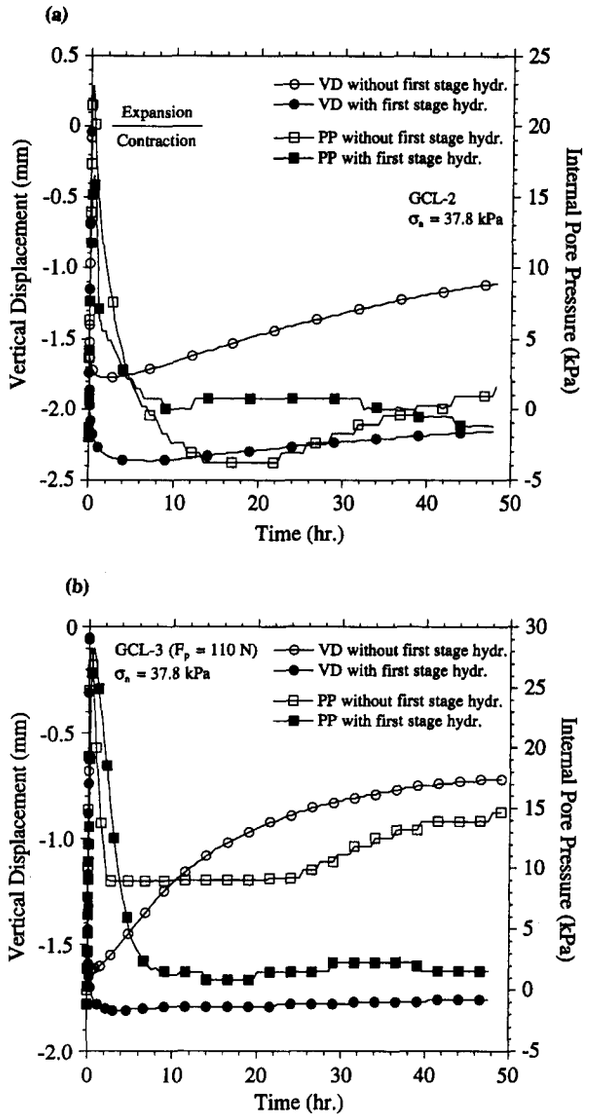

FIG. 2. Vertical Displacement and Internal Pore Pressure during Second-Stage Hydration for: (a) GCL-2; (b) GCL-3

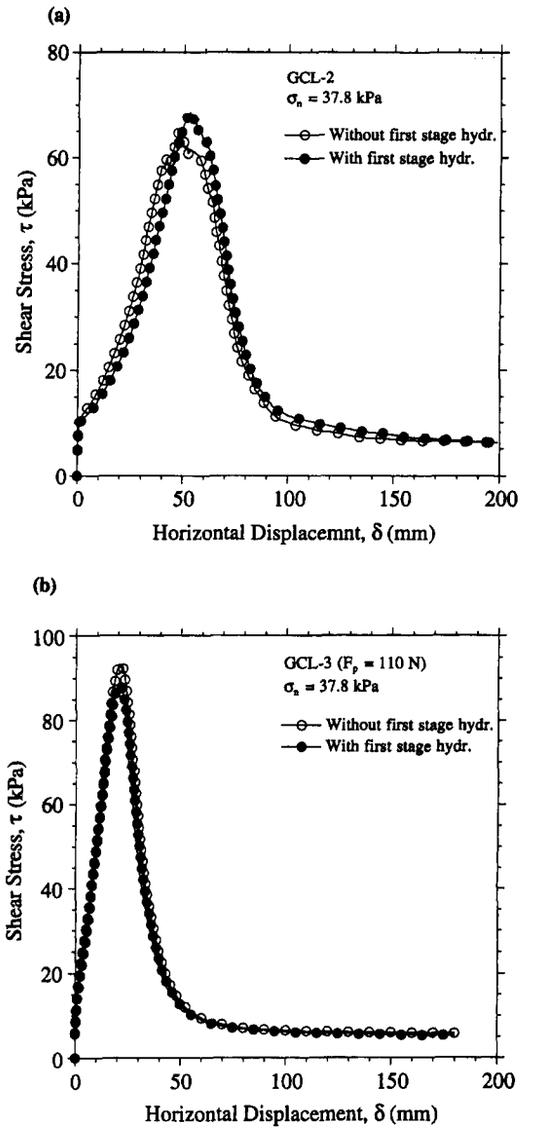

FIG. 3. Stress-Displacement Curves for Hydration Study of: (a) GCL-2; (b) GCL-3

maining tests for the experimental program were conducted using the two-stage hydration procedure.

Fig. 4 shows vertical displacement and internal pore pressure measurements during hydration for the test results presented in Fig. 5 (see next section). Using the two-stage hydration procedure, nearly all tests reached vertical displacement equilibrium within 48 h and many within 24 h. Although the pore pressure measurements were less consistent and the needles may have clogged in some cases (such as for GCL-1 at σ_n = 279 kPa), internal pore pressures dissipated within 48 h for tests at low σ_n but sometimes were not fully dissipated within 48 h for tests at high σ_n (possibly because of the lower hydraulic conductivity of the bentonite).

Stress-Displacement Behavior

Direct shear tests were performed for a normal stress range of 6.9–279 kPa. At low σ_n, some reinforced specimens slipped on the gripping surfaces and could not be sheared internally. The τ versus δ curves for specimens of GCL-1, GCL-2, and GCL-3 (F_p = 160 N) for which internal failures did occur are shown in Fig. 5. Each curve displays marked strain softening with well-defined peak (τ_p) and residual (τ_r) shear strengths. For each test, the value of τ_r was taken as the lowest shear stress recorded after τ_p. In some cases, τ_r was not reached until the very end of the test. Thus, the values of τ_r reported here may not be true residual strengths for which no further decrease occurs with additional displacement. However, shear stress values at large displacements varied only slightly, suggesting that residual conditions were closely approached.

The τ_r/τ_p ratio for each product is plotted versus σ_n in Fig. 6. As might be expected, the reinforced products experienced the most strain softening. Depending on σ_n, GCL-3 lost 92–96% of its shear strength in the transition from peak to residual conditions. GCL-2 showed less strain softening, with τ_r/τ_p increasing from 6 to 29% with increasing normal stress. For GCL-1, τ_r/τ_p varied from 40 to 47% and shows no consistent trend with σ_n.

Fig. 7 shows horizontal displacements at τ_p and $1.1\tau_r$ versus σ_n. Displacements at $1.1\tau_r$ are presented (instead of displacements at τ_r) to avoid the effect of minor fluctuations in shear stress near the end of each test. For GCL-1, τ_p occurred at 1.4–2.4 mm of displacement. GCL-2 required the largest displacement to reach τ_p, between 40 and 63 mm. GCL-3 reached τ_p at 21–26 mm of displacement. The data in Fig. 7 indicate that, with the exception of GCL-2 at low σ_n, a horizontal displacement of 140 mm was sufficient to reach a shear stress within 10% of τ_r. The displacements at τ_p shown in Fig. 7 are somewhat larger than values generally reported for these prod-

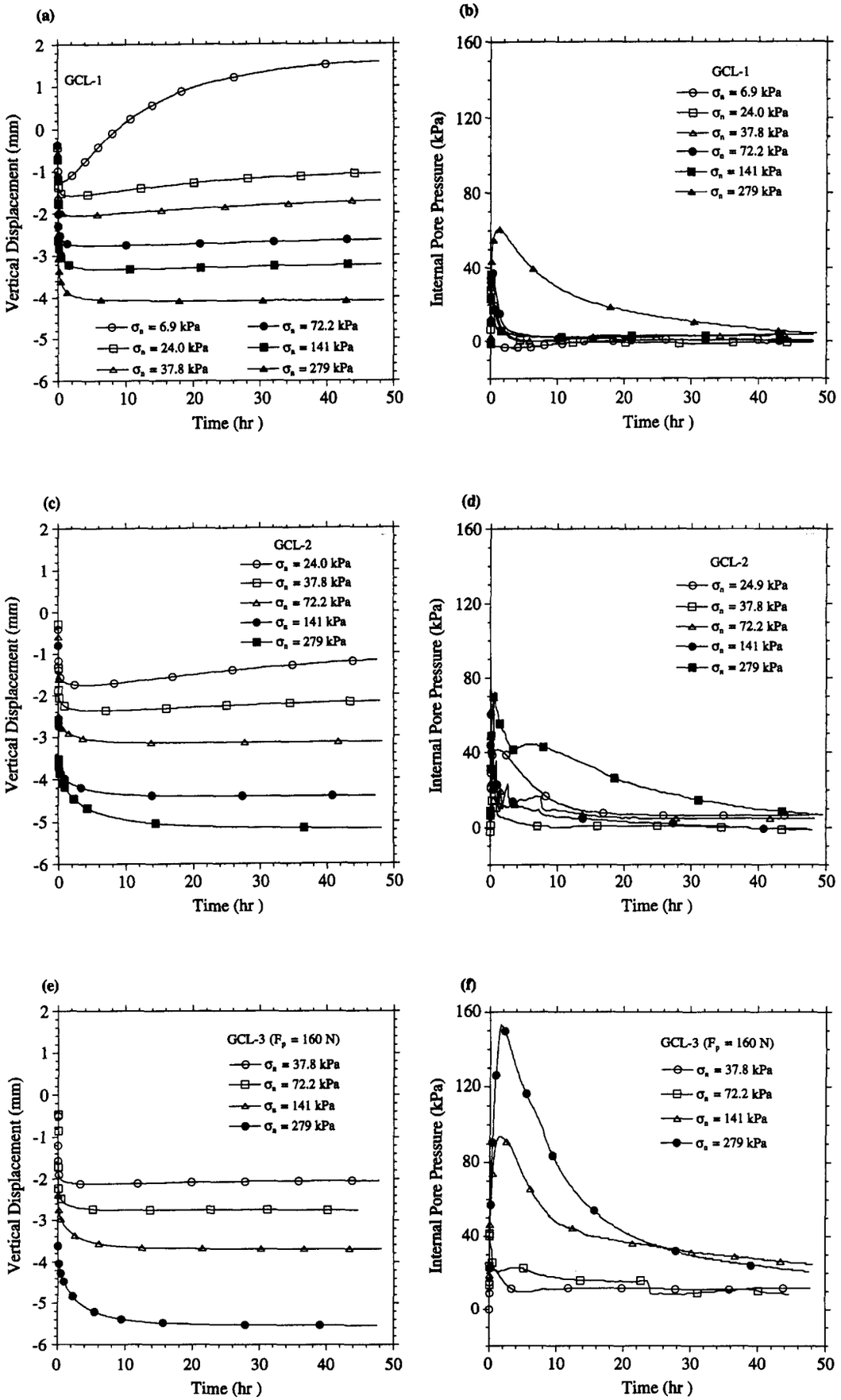

FIG. 4. Specimen Hydration Data: (a) Vertical Displacement, GCL-1; (b) Internal Pore Pressure, GCL-1; (c) Vertical Displacement, GCL-2; (d) Internal Pore Pressure, GCL-2; (e) Vertical Displacement, GCL-3; (f) Internal Pore Pressure, GCL-3

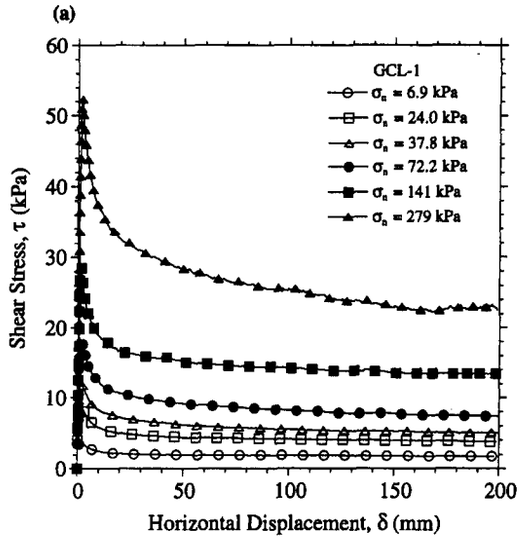

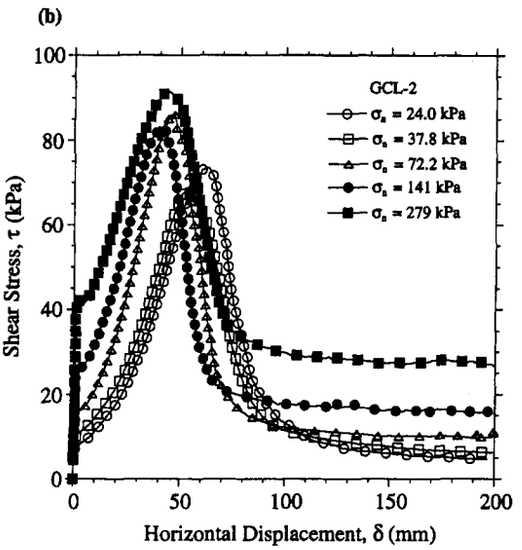

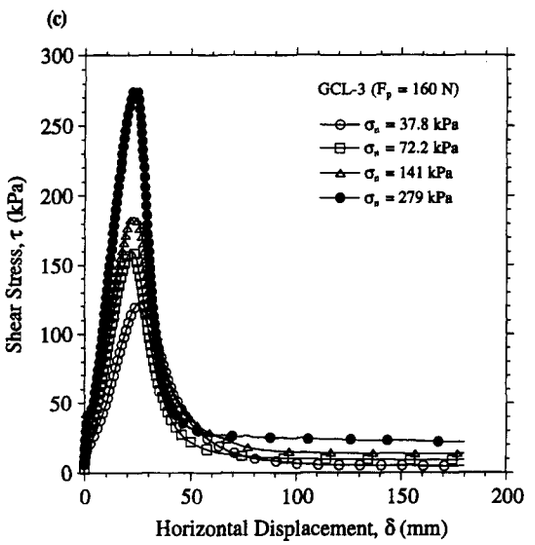

FIG. 5. Stress-Displacement Curves for: (a) GCL-1; (b) GCL-2; (c) GCL-3

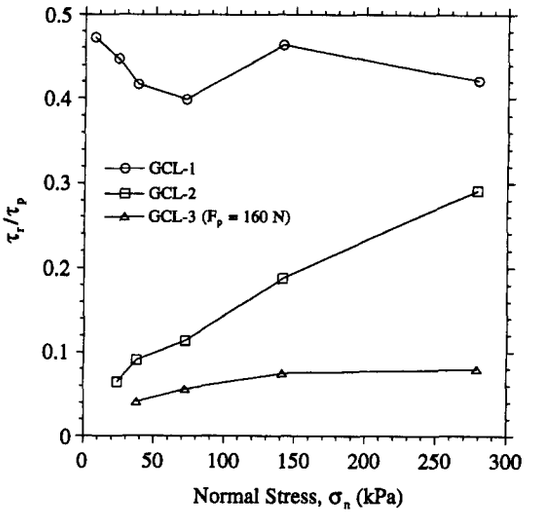

FIG. 6. τ_r/τ_p for Three GCL Products

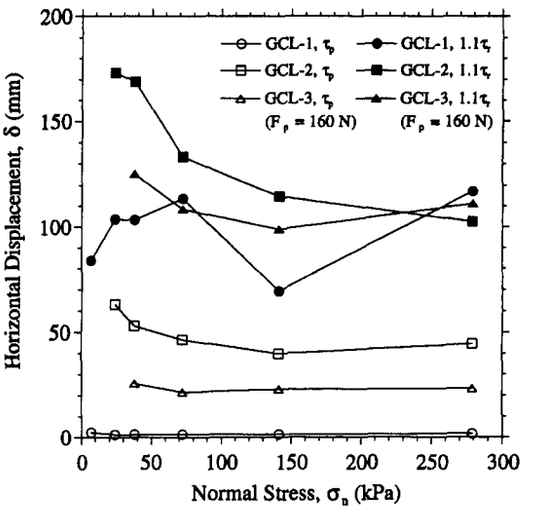

FIG. 7. Horizontal Displacements at τ_p and 1.1τ_r for Three GCL Products

ucts. Although posttest inspections of the failed specimens gave no evidence of slipping of the geotextiles during shear, larger displacements may have been needed to mobilize peak shear strengths in this study because the carrier geotextiles were not clamped to the shearing surfaces. Interestingly, these data may be more representative of field conditions considering that GCLs are not firmly attached to adjacent interfaces during installation.

Shear-induced volume change of the GCL specimens is summarized in Fig. 8. Vertical displacements at τ_p and τ_r are plotted versus σ_n, with each value representing the change in vertical displacement from the beginning of shear. Each GCL product displayed a similar trend of increasingly contractive behavior with increasing σ_n. At peak strength, specimens of GCL-1 experienced essentially no volume change. Corresponding values for the reinforced products were significantly larger. GCL-2 expanded at low σ_n and contracted at high σ_n, whereas GCL-3 contracted at all stress levels (likely because of tension developed in the needle-punched fibers). From τ_p to τ_r, the behavior of GCL-1 and GCL-3 changed from expansive to contractive as σ_n increased. Each specimen of GCL-2 decreased in volume after τ_p. Qualitatively, Fig. 8 illustrates that GCLs exhibit volume change characteristics similar to those for natural clays in direct shear.

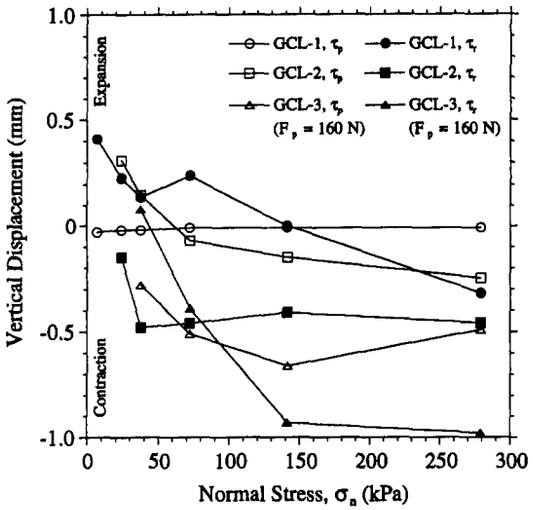

FIG. 8. Vertical Displacements at τ_p and τ_r for Three GCL Products

Shear Strength

The peak shear-strength failure envelope for each GCL product is shown in Fig. 9(a). Four additional tests were performed on specimens of GCL-3 with an average F_p = 85 N, and this envelope also is shown. Individual peel strengths could not be obtained for these specimens due to the limited supply of material. Replicate tests of GCL-2 [not shown in Fig. 5(b)] also were performed at σ_n = 72.2 and 279 kPa to better define the peak strength envelope for this product.

GCL-1 had the lowest peak shear strength at any normal stress. The measured values are in close agreement with published data for unreinforced GCLs (Shan and Daniel 1991; Daniel et al. 1993). The peak strength of GCL-2 increased with normal stress for $\sigma_n < 72$ kPa and was nearly constant at approximately 91 kPa for $\sigma_n > 72$ kPa. For GCL-3, τ_p increased sharply with σ_n and showed a good correlation with F_p. The peak strengths for GCL-2 and GCL-3 generally are larger than corresponding values reported from previous studies. The discrepancies presumably reflect real differences in the GCL products at the time of testing, as well as differences in testing apparatus and procedures.

Each peak strength envelope shows modest nonlinearity and, following the method of Giroud et al. (1993), is described as a p-order hyperbola with nonorthogonal asymptotes. The general equation is

$$\tau_p = a_\infty + \sigma_n \tan \delta_\infty - \frac{a_\infty - a_o}{\left(1 + \frac{\sigma_n}{\sigma_o}\right)^p} \quad (1)$$

where a_∞, δ_∞, a_o, σ_o, and p = constants. Eq. (1) characterizes nonlinear variations of shear strength with respect to normal stress without forcing the relationships through the origin. This is advantageous for reinforced products because, as indicated by peel tests, $\tau_p > 0$ at $\sigma_n = 0$. The peak strength data also can be approximated using linear relationships, shown as dashed lines in Fig. 9(a). To be conservative, each line was drawn between the endpoints of the nonlinear curves using the following equation:

$$\tau_p = c + \sigma_n \tan \phi \quad (2)$$

where c and ϕ = constants. Table 3 lists the peak shear-strength parameters, describing linear and nonlinear failure envelopes, over the applicable normal stress range for each GCL product.

Residual shear strengths for all three products are shown in Fig. 9(b). The data are in close agreement, indicating that stitch-bonded and needle-punched reinforcement does not affect τ_r. Nonlinear and linear envelopes were fitted to the data in the same fashion as for τ_p, giving the following equations:

$$\tau_r = 3.9 \text{ kPa} + \sigma_n \tan 4.1° - \frac{3.9 \text{ kPa}}{\left(1 + \frac{\sigma_n(\text{kPa})}{54.4 \text{ kPa}}\right)^{2.8}}$$

GCL-1, GCL-2, GCL-3 ($7 \le \sigma_n \le 279$ kPa) (3)

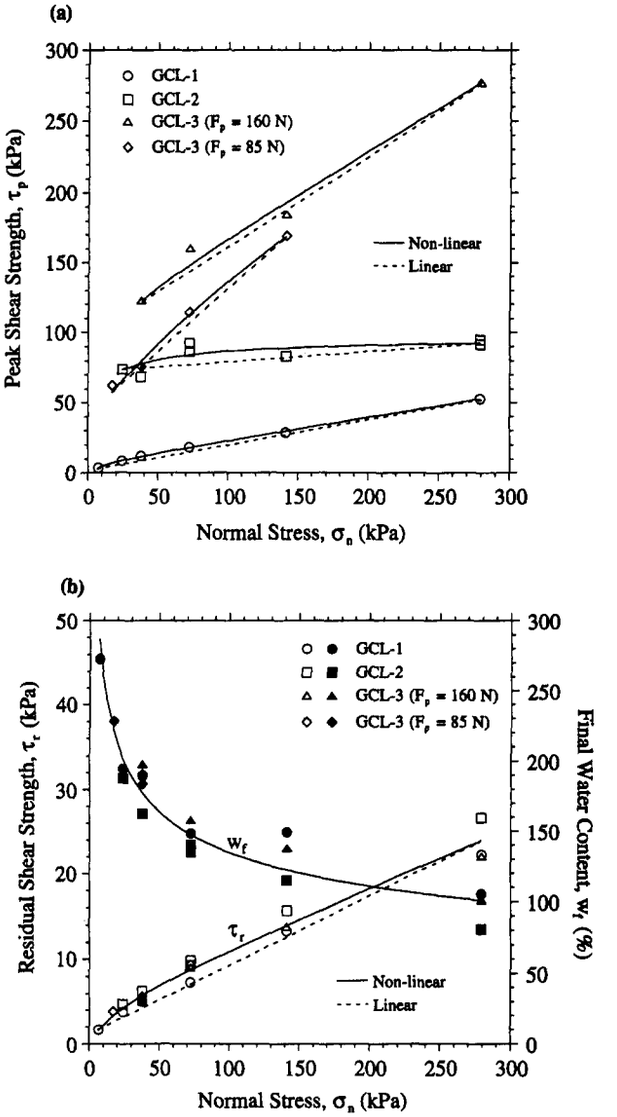

FIG. 9. Failure Envelopes for: (a) Peak Shear Strength; (b) Residual Shear Strength

TABLE 3. Peak Shear-Strength Failure Envelope Parameters

GCL product (1)	Normal stress range, σ_n (kPa) (2)	Nonlinear Envelope a_∞ (kPa) (3)	δ_∞ (°) (4)	a_o (kPa) (5)	σ_o (kPa) (6)	p (7)	Linear Envelope c (kPa) (8)	ϕ (°) (9)
GCL-1	7–279	6.3	9.4	0.5	38	2.5	2.4	10.2
GCL-2	24–279	88	1.0	60	180	5.0	71.6	4.3
GCL-3 (F_p = 160 N)	38–279	112	30.6	86	189	4.3	98.2	32.6
GCL-3 (F_p = 85 N)	17–141	110	31.8	37	177	1.6	42.3	41.9

$$\tau_r = 1.0 \text{ kPa} + \sigma_n \tan 4.7°$$

GCL-1, GCL-2, GCL-3 ($7 \leq \sigma_n \leq 279$ kPa) (4)

The value of $\phi = 4.7°$ for the linear residual strength envelope is in good agreement with the value of 4.0° measured from ring-shear tests on sodium montmorillonite (Müller-Vonmoos and Løken 1989). Linear regression through the τ_r data gives an even closer value of $\phi = 4.4°$.

Also shown in Fig. 9(b), the average final water content (w_f) decreased with increasing σ_n. The approximate relationship obtained from a power law regression is

$$w_f\% = 494(\sigma_n(\text{kPa}))^{-0.282}$$

GCL-1, GCL-2, GCL-3 ($7 \leq \sigma_n \leq 279$ kPa) (5)

Combining (4) and (5), τ_r also can be expressed as

$$\tau_r = 1.0 \text{ kPa} + \left(\frac{w_f\%}{494}\right)^{-3.55} \tan 4.7°$$

GCL-1, GCL-2, GCL-3 ($7 \leq \sigma_n \leq 279$ kPa) (6)

Eq. (6) gives τ_r in terms of final water content of a hydrated GCL specimen after shearing at 0.1 mm/min. Although differences in displacement rate and availability of water during shear may affect this relationship, (6) may be useful as a means to estimate τ_r for failure investigations in which representative values of GCL water content are known.

Effect of Displacement Rate

The effect of horizontal displacement rate on measured shear strength was investigated for GCL-2 and GCL-3 (F_p = 160 N) at $\sigma_n = 72.2$ kPa. Tests were performed using displacement rates of 0.01, 0.1, 1, and 10 mm/min, which bracket the range of displacement rates typically used in practice for shear testing of GCLs. Fig. 10(a) shows τ_p decreased approximately 3.4 and 3.8 kPa per log cycle of displacement rate for GCL-2 and GCL-3, respectively. Fig. 10(b) shows a similar trend for τ_r, with values decreasing approximately 0.48 kPa per log cycle of displacement rate. For both products, τ_p and τ_r decreased approximately 3–5% of the corresponding values at 0.1 mm/min per log cycle of displacement rate. Fig. 10 indicates that, for $\sigma_n = 72.2$ kPa, displacement rate had a relatively small effect on measured shear strength for GCL-2 and GCL-3. In addition, the τ versus δ curves obtained using the different rates were nearly identical for each GCL product (Scheithe 1996; Rowland 1997).

A decrease of shear strength with decreasing displacement rate may result from changes in effective stress on the failure plane (i.e., varying shear-induced excess pore pressures) or creep of the bentonite and/or geosynthetic components during shear. Because τ_r was dependent on displacement rate and excess pore pressures on the failure surfaces were zero (see next section), drained creep of the bentonite appears to be an important, if not the dominant, factor. The trends shown in Fig. 10 are consistent with the results of previous investigations, which indicate a general decrease in measured shear strength with decreasing displacement rate for both unreinforced and reinforced GCLs (Daniel et al. 1993; Stark and Eid 1996; Gilbert et al. 1997). However, differences in product types, testing apparatus, and testing procedures have resulted in different magnitudes of measured strength decrease. Additional research on the effect of displacement rate on measured shear strength under varying normal stress conditions is warranted.

Shear-Strength Mechanisms

The failure plane for each GCL product was located at the woven geotextile/bentonite interface and not within the hydrated bentonite. During shear, the upper geotextile was pulled off the top of each specimen while additional geotextile was drawn in the rear of the test chamber with the pullout plate. Some specimens of GCL-1 have failed at the bottom woven geotextile/bentonite interface in previous tests. For each test, the interface pore pressure needle recorded essentially zero (±0.7 kPa) excess pore pressure at the failure surface during shear. The effective normal stress on the failure plane was therefore equal to the applied vertical stress and the measured shear strengths are considered representative of consolidated-drained conditions. The measured values of internal excess pore pressure during shear are questionable. Apparent clogging of the needle and movement of the needle within the clay resulted in spurious readings for many tests. As a result, vertical effective stresses inside the bentonite cannot be calculated reliably from the internal pore pressure data (Scheithe 1996; Rowland 1997).

The mode of failure for GCL-1 indicates that the unreinforced woven geotextile/bentonite interface had a lower shear strength than the hydrated bentonite. Strain softening likely resulted from clay particle reorientation on the failure surface and the failure of any water-soluble adhesives that may have been present. For the reinforced products, strain softening was

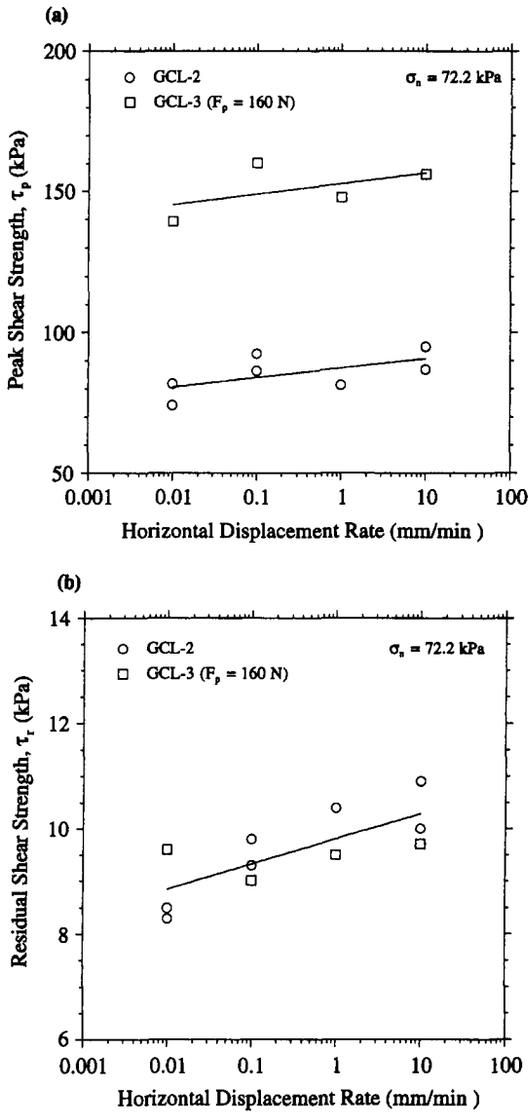

FIG. 10. Effect of Horizontal Displacement Rate on Shear Strength of Reinforced GCLs: (a) τ_p; (b) τ_r

more pronounced because of failure of the geosynthetic components. Fig. 11 shows failed specimens of GCL-2 and GCL-3 at σ_n = 279 and 72.2 kPa, respectively. Failure of GCL-2 occurred as the reinforcing stitches pulled through the upper geotextile, creating four longitudinal rips at the locations of the lines of stitching. The reinforcing stitches themselves remained unbroken and connected to the woven geotextile/laminated geomembrane. Thus, the peak shear strength of GCL-2 was controlled by the strength of the woven geotextile and not by the strength of the stitches. Damage to the geomembrane of GCL-2 as a result of shear was not observed for any of the tests conducted. Similar to the observations of Gilbert et al. (1996a), specimens of GCL-3 failed as the majority of reinforcing fibers pulled out of the woven geotextile. In addition, some fibers broke or pulled out of the nonwoven geotextile. Migration of hydrated bentonite through the woven geotextiles also was observed for all three GCL products after the specimens were removed from the shear machine.

A comparison of stress-displacement behavior for the three GCL products gives insight with regard to mechanisms of shear-strength mobilization. Fig. 12 shows τ versus δ for each product at σ_n = 141 kPa. A detail of the initial portion of these curves is shown in the upper right corner. For $\delta \leq 1$ mm, each product displayed a similar increase in shear stress with horizontal displacement. Thus, the initial mobilized shear strength of the woven geotextile/bentonite interface was independent of reinforcement. For $\delta > 1$ mm, the curves diverge. GCL-1 failed at δ = 1.4 mm, whereas GCL-2 and GCL-3 began to mobilize their reinforcement and eventually reached larger peak strengths. The horizontal displacement at τ_p was greater for GCL-2 (δ = 39.7 mm) than for GCL-3 (δ = 22.9 mm)

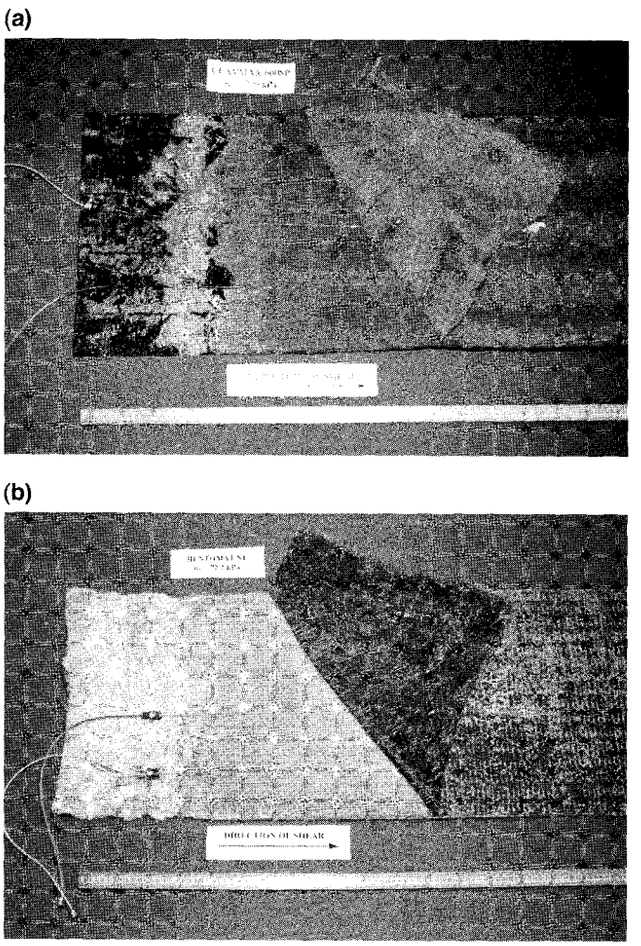

FIG. 11. Failed Specimens of: (a) GCL-2 at σ_n = 279 kPa; (b) GCL-3 at σ_n = 72.2 kPa

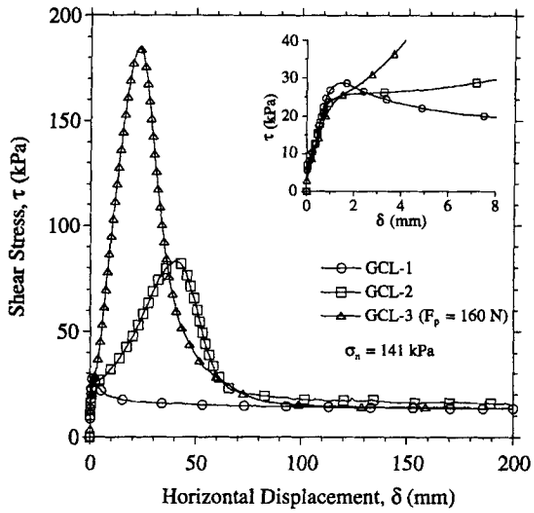

FIG. 12. Stress-Displacement Curves for Three GCL Products at σ_n = 141 kPa

because of differences in the area of reinforcement relative to total specimen area for these products. For GCL-2, the upper woven geotextile stretched around the stitching, giving a larger displacement at τ_p [an example is shown in Fig. 6 of Fuller (1995)]. Specimens of GCL-3 failed at smaller displacements because of the uniform coverage of the needle-punched fibers. After peak strength was reached, the shear strength for all three specimens decreased to residual values that essentially were independent of product type.

The contribution of reinforcement to the peak shear strength of GCL-2 and GCL-3 is shown as a function of normal stress in Fig. 13. To prepare this plot, postpeak shear strengths of GCL-1 (τ_{GCL-1}) were subtracted from peak shear strengths of GCL-2 and GCL-3 at corresponding values of horizontal displacement. For example (see Fig. 12), the contribution of stitch-bonded reinforcement to the peak strength of GCL-2 at σ_n = 141 kPa was obtained by subtracting τ_{GCL-1} = 15.8 kPa (δ = 39.7 mm) from τ_p = 83.2 kPa (δ = 39.7 mm), giving a value of 67.4 kPa. Fig. 13 shows the additional shear strength contributed by the stitch-bonded reinforcement for GCL-2 was essentially independent of σ_n and therefore solely dependent on the strength of the woven geotextile. In addition, the data suggest that the increase of τ_p with σ_n for GCL-2 [Fig. 9(a)] was caused by the increased shear strength of the woven geotextile/bentonite interface rather than of the reinforcement. For

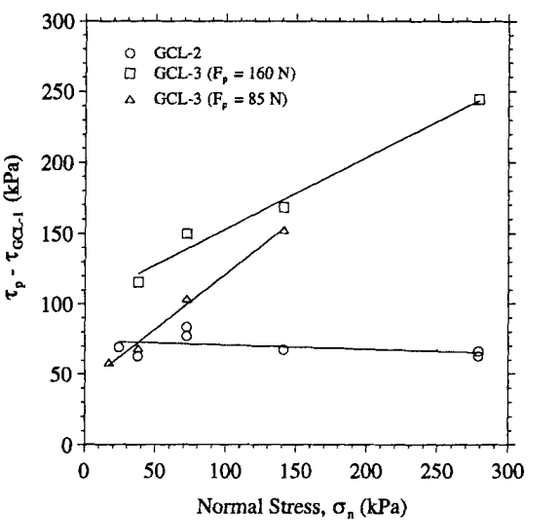

FIG. 13. Contribution of Reinforcement to Peak Shear Strength of GCL-2 and GCL-3

GCL-3, the additional shear strength gained from the needle-punched reinforcement increased significantly with σ_n and displayed a clear correlation with peel strength. This finding lends support to the hypothesis proposed by Gilbert et al. (1996a) that fiber connections for GCL-3 are frictional in nature. The failure mechanism for GCL-3 also suggests that, as σ_n increases, the majority of fibers may begin to break instead of pull out from the woven geotextile. In this case, the additional shear strength provided by the reinforcement for GCL-3 would, like GCL-2, be essentially independent of normal stress. However, failure envelopes for two needle-punched GCLs presented by Richardson (1997) show no significant change in tangent friction angle for σ_n = 80–1,200 kPa.

The peak shear strength of GCL-2 was found to be dependent on the direction of shear. Shown schematically in Fig. 14, the stitch type is classified as a 101 single-thread chain stitch, which is formed by the penetration of a needle thread loop through the product such that it passes through the previous loop on the other side (Ko 1987). When shear stress was applied in the "standard" direction (i.e., the direction of stitch formation), the stitches locked and failure occurred when the lines of stitching ripped through the woven geotextile. When shear stress was applied in the "reverse" direction, the stitches progressively unraveled and the peak shear strength was reduced. Fig. 15 shows the effect of shear direction on the stress-displacement response of GCL-2 at σ_n = 72.2 kPa. Although the curves are nearly identical for $\delta \leq 30$ mm, the average peak shear strength of the reverse specimens was less than that of the standard specimens by a factor of 1.8 (i.e., 43%). Examination of the reverse specimens after testing showed that

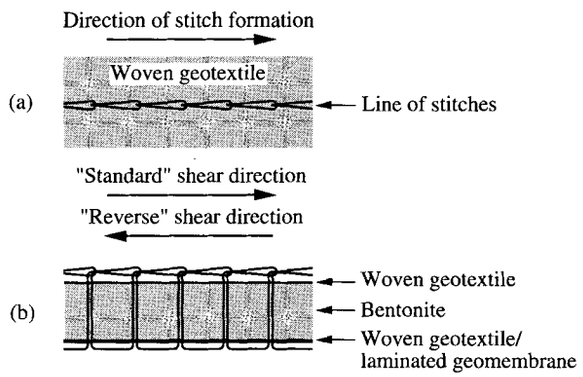

FIG. 14. Schematic Diagram of Stitch-Bonded Reinforcement for GCL-2: (a) Plan View; (b) Profile View

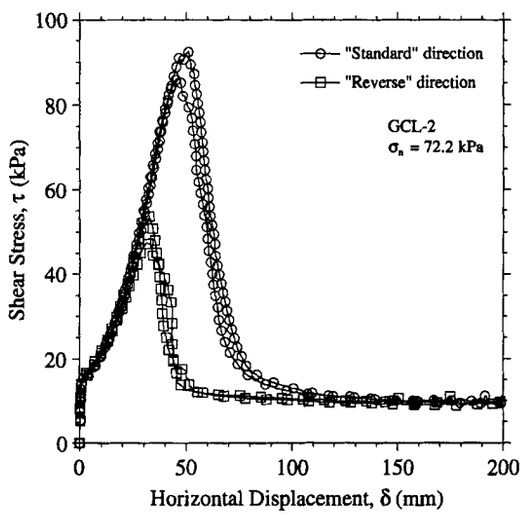

FIG. 15. Stress-Displacement Curves for GCL-2 Sheared in Standard and Reverse Directions

the failure surface was again located at the woven geotextile/bentonite interface. However, both the woven geotextile and the stitch yarn remained intact; the stitching loops simply pulled through the geotextile progressively without tearing it. At this time, it is unknown if similar stitch unraveling could occur in the field. Until further information becomes available it is recommended that GCL-2 be tested and/or installed such that shear stresses are aligned in the standard direction of the product.

COMMENTS

The shear strength of GCLs is an important consideration for design because these products commonly are expected to withstand transient in-plane shear stresses during construction and, in some cases, permanent shear stresses over the life of a facility. This paper has presented experimental data on peak and residual internal shear strengths of adhesive-bonded, stitch-bonded, and needle-punched GCLs. The information has implications for the design of waste-containment facilities and other facilities incorporating GCLs and for the manufacturing and testing of GCL products.

Each GCL product is strain softening in direct shear. The reduction of shear strength from peak to residual is dependent on reinforcement type. GCL-1 has the smallest peak strength and experiences a postpeak strength loss of approximately 55%. As a general guideline, unreinforced GCLs are not recommended for slopes steeper than 10H:1V (CETCO 1995; Frobel 1996; Richardson 1997). Based on τ_p and a normal stress range of 7–279 kPa, GCL-1 would provide a safety factor of approximately 1.8 (=10 tan 10.2°) for an infinite 10H:1V slope without seepage (assuming hydrated conditions and c = 0). Using τ_r, the safety factor decreases to less than 1. At low σ_n, the peak strengths of GCL-2 and GCL-3 are comparable. As σ_n increases, GCL-3 is the stronger product. GCL-3 (F_p = 160 N) also shows the most strain softening; over 90% of the peak strength is lost at large displacements. From an internal stability standpoint, GCL-2 and GCL-3 probably are suited equally for low σ_n applications (e.g., pond liners and cover systems), whereas GCL-3 is probably the better choice for high σ_n applications (e.g., bottom liners). The stress-displacement behavior of each GCL product can be characterized in terms of peak and residual shear strengths (Fig. 9) and their corresponding displacements (Fig. 7). Such information is needed for stability analyses which account for strain-softening materials and progressive failure effects (Byrne 1994; Gilbert et al. 1996b). Clearly, a key issue with regard to internal stability of GCLs is residual shear strength. If the safety factor using τ_r is unacceptable, a designer must evaluate the likelihood for developing residual-shear conditions internally within the GCL and, if necessary, the risk posed by such conditions.

Better knowledge of GCL internal failure mechanisms can lead to improved product performance and/or reductions in the cost of manufacturing. The peak shear strength of GCL-2 may be increased by incorporating a stronger woven geotextile. Likewise, using a different type of stitch for GCL-2 may eliminate the dependence of peak strength on shear direction. The peak strength of GCL-3 may be improved by strengthening the connection of the needle-punched fibers with the woven geotextile. The residual shear strength of each product only can be improved by increasing the residual shear strength of the woven geotextile/bentonite interface. One possibility might be to incorporate a granular admixture (e.g., sand) into the bentonite layer (Fox 1998). In a related study, Schmitt et al. (1997) found that the small displacement shear strength ($\delta \leq$ 10 mm) of sodium bentonite can be increased by mixing it with granular expanded shale.

The findings of the study have implications with regard to

direct shear testing of GCLs. The two-stage hydration procedure may reduce in-machine hydration time and allow for more efficient use of test equipment. In this study, horizontal displacement rate had a small effect on measured peak and residual shear strengths for the reinforced products. Because failure did not occur within the hydrated bentonite, displacement rates estimated from GCL consolidation data appear to have little relevance. This may allow drained shear tests to be performed at rates faster than those currently prescribed by ASTM D 3080 (ASTM 1996), reducing the cost of performance testing for GCLs. Measured shear strengths then can be corrected for displacement rate once more information becomes available on this effect. Using Figs. 7 and 9(b), laboratories with direct shear apparatus smaller than the pullout shear machine may assess the quality of measured residual shear strengths. Ring-shear data may be helpful in this regard for some products (Stark and Eid 1996). Data from this study also show that specimens of GCL-2 must be sheared in the standard direction to obtain consistent results in the laboratory.

Finally, the location of a potential failure surface is controlled by the internal shear strength of a GCL and the interface shear strengths between a GCL and adjacent materials. As indicated by failures of the Cincinnati test plots (Koerner et al. 1996) and a landfill cover system incorporating a stitch-bonded GCL (U.S. Environmental Protection Agency 1996), interface failures are more likely for reinforced products at low σ_n. At high σ_n, internal strength may become the limiting factor, causing the failure plane to move into the GCL (Gilbert et al. 1996a). Thus, the potential for both internal and interface failures must be evaluated for designs that incorporate GCLs. The internal shear-strength data presented in this paper should not be used in place of product-specific testing under conditions matching those expected in the field.

CONCLUSIONS

The following conclusions are reached as a result of this investigation of the internal shear strength of adhesive-bonded, stitch-bonded, and needle-punched GCLs:

1. Peel tests provided a useful indication of relative peak shear strength for the needle-punched GCL. Peel tests could not be performed reliably on specimens of the stitch-bonded product.
2. A 4-day, two-stage hydration procedure, in which a GCL specimen is hydrated to the estimated final water content 2 days prior to the application of normal stress, reduced the required in-machine hydration time to reach equilibrium conditions and allowed for more efficient use of testing equipment. In a limited number of comparative tests, the procedure did not alter the internal shear strength of reinforced GCLs.
3. The failure surface was located at the woven geotextile/bentonite interface for each test performed. The stitch-bonded product failed as the lines of stitching ripped through the woven geotextile. For the needle-punched product, the majority of reinforcing fibers pulled out of the woven geotextile during shear.
4. The peak shear-strength (τ_p) failure envelope was modestly nonlinear for each GCL product. At any given normal stress (σ_n), the magnitude of τ_p was a function of reinforcement type. The adhesive-bonded GCL was weakest at all stress levels. At low σ_n, peak strengths for the stitch-bonded and needle-punched products were comparable. As σ_n increased, the needle-punched GCL was the stronger product.
5. The residual shear-strength (τ_r) failure envelope was modestly nonlinear and independent of product type. The test data also showed a good correlation between τ_r and final GCL water content.
6. Excess pore pressures remained at zero on the failure plane of each specimen during shear. The effective normal stress on the failure plane was therefore equal to the applied vertical stress, and the failure envelopes for τ_p and τ_r are considered representative of consolidated-drained conditions.
7. The contribution of needle-punched reinforcement to peak shear strength increased with σ_n. The contribution of stitch-bonded reinforcement to peak strength essentially was independent of σ_n.
8. Peak shear strength of the stitch-bonded product was dependent on the direction of shear. At σ_n = 72.2 kPa, τ_p varied by a factor of 1.8 for specimens sheared in opposite directions.
9. A horizontal displacement of approximately 1.5 mm was required to reach τ_p for the adhesive-bonded product. The stitch-bonded and needle-punched products required significantly larger displacements (40–63 mm and 17–26 mm, respectively) to mobilize peak shear strength.
10. For most tests, a horizontal displacement of 140 mm was sufficient to reach a shear stress within 10% of τ_r.
11. For the reinforced products at σ_n = 72.2 kPa, τ_p and τ_r decreased approximately 3–5% of the corresponding values at 0.1 mm/min per log cycle of displacement rate. In general, displacement rate had a relatively small effect on measured shear strengths for this study.

ACKNOWLEDGMENTS

This investigation was supported financially by CETCO; Grant No. CMS-9309566 from the Geomechanical, Geotechnical, Geoenvironmental Systems Program of the U.S. National Science Foundation; and the Bechtel Foundation. This financial support is gratefully acknowledged. The writers thank Eric Triplett for his assistance with the experimental program, as well as Richard Carriker, Jim Olsta, and Robert Trauger for their support and assistance with the project. The views expressed in this paper are solely those of the writers and no endorsement by the sponsors is implied.

APPENDIX I. REFERENCES

ASTM. (1996). "Standard test method for direct shear test of soils under consolidated drained conditions." *Annual book of ASTM standards, ASTM D 3080*, Vol. 04.08, ASTM, West Conshohocken, Pa., 295–300.

ASTM. (1997). "Standard test method for grab breaking load and elongation of geotextiles." *Annual book of ASTM standards, ASTM D 4632*, Vol. 04.09, ASTM, West Conshohocken, Pa., 972–975.

Byrne, R. J. (1994). "Design issues with strain-softening interfaces in landfill liners." *Proc., Waste Tech. '94*, Charleston, S.C., 1–26.

Colloid Environmental Technologies Co. (CETCO). (1995). *Bentomat/Claymax technical manual*. CETCO, Arlington Heights, Ill.

Daniel, D. E., Shan, H.-Y., and Anderson, J. D. (1993). "Effects of partial wetting on the performance of the bentonite component of a geosynthetic clay liner." *Proc., Geosynthetics '93*, Vol. 3, Industrial Fabrics Assoc. Int., Roseville, Minn., 1483–1496.

Fox, P. J. (1998). "Research on geosynthetic clay liners at Purdue University." *Geotech. News*, Vancouver, Canada, 16(1), 35–40.

Fox, P. J., Rowland, M. G., Scheithe, J. R., Davis, K. L., Supple, M. R., and Crow, C. C. (1997). "Design and evaluation of a large direct shear machine for geosynthetic clay liners." *Geotech. Testing J.*, 20(3), 279–288.

Frobel, R. K. (1996). "Geosynthetic clay liners, part four: Interface and internal shear strength determination." *Geotech. Fabrics Rep.*, Industrial Fabrics Assoc. Int., Roseville, Minn., 14(8), 20–23.

Fuller, J. M. (1995). "Landfill cap designs using geosynthetic clay liners." *Geosynthetic clay liners*, R. M. Koerner, E. Gartung, and H. Zanzinger, eds., A. A. Balkema, Rotterdam, The Netherlands, 129–140.

Gilbert, R. B., Fernandez, F., and Horsfield, D. W. (1996a). "Shear strength of reinforced geosynthetic clay liner." *J. Geotech. Engrg.*, ASCE, 122(4), 259–266.

Gilbert, R. B., Long, J. H., and Moses, B. E. (1996b). "Analytical model

of progressive slope failure in waste containment systems." *Int. J. for Numer. and Analytical Methods in Geomech.*, 20(1), 35–56.
Gilbert, R. B., Scranton, H. B., and Daniel, D. E. (1997). "Shear strength testing for geosynthetic clay liners." *Testing and acceptance criteria for geosynthetic clay liners*, STP 1308, L. W. Well, ed., ASTM, West Conshohocken, Pa., 121–135.
Giroud, J. P., Darrasse, J., and Bachus, R. C. (1993). "Hyperbolic expression for soil-geosynthetic or geosynthetic-geosynthetic interface shear strength." *Geotextiles and Geomembranes*, England, 12(3), 275–286.
Heerten, G., Saathoff, F., Scheu, C., and von Maubeuge, K. P. (1995). "On the long-term shear behavior of geosynthetic clay liners (GCLs) in capping sealing systems." *Geosynthetic clay liners*, R. M. Koerner, E. Gartung, and H. Zanzinger, eds., A. A. Balkema, Rotterdam, The Netherlands, 141–150.
Ko, F. K. (1987). "Seaming and joining methods." *Geotextiles and Geomembranes*, England, 6(1–3), 93–107.
Koerner, R. M. (1997). "Perspectives on geosynthetic clay liners." *Testing and acceptance criteria for geosynthetic clay liners*, STP 1308, L. W. Well, ed., ASTM, West Conshohocken, Pa., 3–20.
Koerner, R. M., Carson, D. A., Daniel, D. E., and Bonaparte, R. (1996). "Current status of the Cincinnati GCL test plots." *Proc., GRI-10, Field Perf. of Geosynthetics and Geosynthetic Related Sys.*, Drexel University, Philadelphia, Pa., 147–175.
Müller-Vonmoos, M., and Løken, T. (1989). "The shearing behavior of clays." *Appl. Clay Sci.*, Amsterdam, 4(2), 125–141.
Richardson, G. N. (1997). "GCL internal shear strength requirements." *Geotech. Fabrics Rep.*, Industrial Fabrics Assoc. Int., Roseville, Minn., 15(2), 20–25.
Rowland, M. G. (1997). "Research on the internal shear strength of three geosynthetic clay liners," MS thesis, School of Civil Engineering, Purdue University, West Lafayette, Ind.
Scheithe, J. R. (1996). "Research on the internal shear strength of a needle-punched geosynthetic clay liner," MS thesis, School of Civil Engineering, Purdue University, West Lafayette, Ind.
Schmitt, K. E., Bowders, J. J., Gilbert, R. B., and Daniel, D. E. (1997). "Enhanced shear strength of sodium bentonite using frictional additives." *Proc., Int. Containment Technol. Conf.*, Florida State Univ., Tallahassee, Fla, 355–361.
Shan, H.-Y., and Daniel, D. E. (1991). "Results of laboratory tests on a geotextile/bentonite liner material." *Proc., Geosynthetics '91*, Vol. 2, Industrial Fabrics Assoc. Int., Roseville, Minn., 517–535.
Stark, T. D., and Eid, H. T. (1996). "Shear behavior of reinforced geosynthetic clay liners." *Geosynthetics Int.*, Industrial Fabrics Assoc. Int., Roseville, Minn., 3(6), 771–786.
U.S. Environmental Protection Agency. (1996). "Report of 1995 workshop on geosynthetic clay liners." *Rep. No. EPA/600/R-96/149*, Office of Research and Development, Washington, D.C.

APPENDIX II. NOTATION

The following symbols are used in this paper:

a_∞, δ_∞, a_o, σ_o, p = constants for nonlinear failure envelope equation;
c, ϕ = constants for linear failure envelope equation;
F_p = peel strength;
w_f = final GCL water content;
δ = horizontal displacement;
σ_n = normal stress;
τ = shear stress;
$\tau_{GCL\text{-}1}$ = postpeak shear strength for GCL-1;
τ_p = peak shear strength; and
τ_r = residual shear strength.